

Variable-lag Granger Causality and Transfer Entropy for Time Series Analysis

CHAINARONG AMORNBUNCHORNVEJ, National Electronics and Computer Technology Center
 ELENA ZHELEVA, University of Illinois at Chicago
 TANYA BERGER-WOLF, University of Illinois at Chicago and The Ohio State University

Granger causality is a fundamental technique for causal inference in time series data, commonly used in the social and biological sciences. Typical operationalizations of Granger causality make a strong assumption that every time point of the effect time series is influenced by a combination of other time series with a fixed time delay. The assumption of fixed time delay also exists in Transfer Entropy, which is considered to be a non-linear version of Granger causality. However, the assumption of the fixed time delay does not hold in many applications, such as collective behavior, financial markets, and many natural phenomena. To address this issue, we develop variable-lag Granger causality and Transfer Entropy, generalizations of both Granger causality and Transfer Entropy that relax the assumption of the fixed time delay and allows causes to influence effects with arbitrary time delays. In addition, we propose a method for inferring both variable-lag Granger causality and Transfer Entropy relations. We demonstrate our approach on an application for studying coordinated collective behavior and other real-world casual-inference datasets and show that our proposed approaches perform better than several existing methods in both simulated and real-world datasets. Our approach can be applied in any domain of time series analysis. The software of this work is available in the R package: `VLTimeSeriesCausality`.

CCS Concepts: •**Information systems** → **Spatial-temporal systems; Data mining; •Computing methodologies** → *Cooperation and coordination*;

Additional Key Words and Phrases: Granger Causality, Transfer entropy, Time Series, Causal Inference, Statistical methodology

ACM Reference format:

Chainarong Amornbunchornvej, Elena Zheleva, and Tanya Berger-Wolf. 2020. Variable-lag Granger Causality and Transfer Entropy for Time Series Analysis. *ACM Trans. Knowl. Discov. Data.* 1, 1, Article 1 (January 2020), 24 pages.

DOI: 10.1145/1122445.1122456

1 INTRODUCTION

Inferring causal relationships from data is a fundamental problem in statistics, economics, and science in general. The gold standard for assessing causal effects is running randomized controlled trials which randomly assign a treatment (e.g., a drug or a specific user interface) to a subset of a population of interest, and randomly select another subset as a control group which is not given the treatment, thus attributing the outcome difference between the two groups to the treatment. However, in many cases, running such trials may be unethical, expensive, or simply

Permission to make digital or hard copies of all or part of this work for personal or classroom use is granted without fee provided that copies are not made or distributed for profit or commercial advantage and that copies bear this notice and the full citation on the first page. Copyrights for components of this work owned by others than ACM must be honored. Abstracting with credit is permitted. To copy otherwise, or republish, to post on servers or to redistribute to lists, requires prior specific permission and/or a fee. Request permissions from permissions@acm.org.

© 2020 ACM. 1556-4681/2020/1-ART1 \$15.00

DOI: 10.1145/1122445.1122456

impossible [45]. To address this issue, several methods have been developed to estimate causal effects from observational data [27, 41].

In the context of time series data, a well-known method that defines a causal relation in terms of *predictability* is Granger causality [18]. X Granger-causes Y if past information on X predicts the behavior of Y better than Y 's past information alone [6]. In this work, when we refer to causality, we mean specifically the predictive causality defined by Granger causality. The key assumptions of Granger causality are that 1) the process of effect generation can be explained by a set of structural equations, and 2) the current realization of the effect at any time point is influenced by a set of causes in the past. Similar to other causal inference methods, Granger causality assumes unconfoundedness and that all relevant variables are included in the analysis. There are several studies that have been developed based on Granger causality [7, 24, 29]. The typical operational definitions [7] and inference methods for inferring Granger causality, including the common software implementation packages [1, 2], assume that the effect is influenced by the cause with a fixed and constant time delay.

Granger causality has another assumption of linearity of structural equations that causes influence effects. Hence, *Transfer Entropy* has been developed to be a non-linear extension of Granger causality [9, 23]. However, the assumption of an effect is fixed-lag influenced by the cause still exists in transfer entropy.

This assumption of a fixed and constant time delay between the cause and effect is, in fact, too strong for many applications of understanding natural world and social phenomena. In such domains, data is often in the form of a set of time series and a common question of interest is which time series are the (causal) initiators of patterns of behaviors captured by another set of time series. For example, who are the individuals who influence a group's direction in collective movement? What are the sectors that influence the stock market dynamics right now? Which part of the brain is critical in activating a response to a given action? In all of these cases, effects follow the causal time series with delays that can vary over time.

To address the remaining gap, we introduce the concept *Variable-lag Granger causality* and *Variable-lag Transfer Entropy* and methods to infer them in time series data. We prove that our definitions and the proposed inference methods can address the arbitrary-time-lag influence between cause and effect, while the traditional operationalizations of Granger causality, transfer entropy, and their corresponding inference methods cannot. We show that the traditional definitions are indeed special cases of the new relations we define. We demonstrate the applicability of the newly defined causal inference frameworks by inferring initiators of collective coordinated movement, a problem proposed in [4], as well as inferring casual relations in other real-world datasets.

We use Dynamic Time Warping (DTW) [31] to align the cause X to the effect time series Y while leveraging the power of Granger causality and transfer entropy. In the literature, there are many clustering-based Granger causality methods that use DTW to cluster time series and perform Granger causality only for time series within the same clusters [28, 46]. Previous work on inferring causal relations using both Granger causality and DTW has the assumption that the smaller warping distance between two time series, the stronger the causal relation is [40]. If the minimum distance of elements within the DTW optimal warping path is below a given distance threshold, then the method considers that there is a causal relation between the two time series. However, their work assumes that Granger causality and DTW should run independently. In contrast, our method formalizes the integration of Granger causality and DTW by generalizing the definition of Granger causality itself and using DTW as an instantiation of the optimal alignment requirement of the time series.

In addition to the standard uses of Granger causality, our method is capable of:

- **Inferring arbitrary-lag causal relations:** our method can infer Granger causal relation where a cause influences an effect with arbitrary delays that can change dynamically;
- **Quantifying variable-lag emulation:** our method can report the similarity of time series patterns between the cause and the delayed effect, for arbitrary delays;

We also prove that when multiple time series cause the behavioral convergence of a set of time series then we can treat the set of these initiating causes in the aggregate and there is a causal relation between this aggregate cause (of the set of initiating time series) and the aggregate of the rest of the time series. We provide many experiments and examples using both simulated and real-world datasets to measure the performance of our approach in various causality settings and discuss the resulting domain insights. Our framework is highly general and can be used to analyze time series from any domain.

2 RELATED WORK

Many causal inference methods assume that the data is *i.i.d.* and rely on knowing a mechanism that generates that data, e.g., expressed through causal graphs or structural equations [27]. In time series data, the values of the consecutive time steps violate the *i.i.d.* assumption. Another set of causal inference methods relax the strong *i.i.d.* assumption, and instead assume independence between the cause and the mechanism generating the effect [21, 32, 35]. Specifically, knowing the cause $X = x$ never reveals information about the structural function $f(X)$ and vice versa. This idea has been used in the context of times series data [35] by relying on the concept of Spectral Independence Criterion (SIC). If a cause X is a stationary process that generates the effect Y via linear time invariance filter h (mechanism), then X and h should not contain any information about each other but dependency between them and Y exists in spectral sense.

Granger causality has inspired a lot of research since its introduction in 1969 [18]. Recent work on Granger causality has focused on various generalizations for it, including ones based on information theory, such as transfer entropy [33, 38] and directed information graphs [30]. Recent inference methods are able to deal with missing data [20] and enable feature selection [44]. Granger causality has even been explored as a method to offer explainability of machine learning models [34]. However, none of them study tests for variable-lag Granger causality, as we propose in this work.

There is a framework of causal inference in [25] based on conditional independence tests on time series generated from some discrete-time stochastic processes that allows unknown latent variables. However, the approach in [25] still assumes that data points at any time step have been generated from some structural vector autoregression (SVAR). The recent work in [19] models causal relation between time series as a form of polynomial function and uses a stochastic block model to find a causal graph. Both works, however, still have the assumption of fixed-lag influence from causes to effects.

Besides, no method studies a causal structure that is unstable overtime [15]. Moreover, Transfer Entropy, which is considered to be a non-linear extension of Granger causality [9, 23], still has the fixed-lag assumption.

In our work, we also relax the stationary assumption of time series.

3 EXTENSION FROM PREVIOUS WORK

This paper is an extension of our conference proceeding [5]. According to our previous work [5], we formalized a VL-Granger causality and proposed a framework to infer a causal relation using BIC and F-test as main criteria to infer whether X causes Y . However, in this work, we propose to use a *Bayesian Information Criterion difference ratio* as a main criterion. Hence, we rerun all results

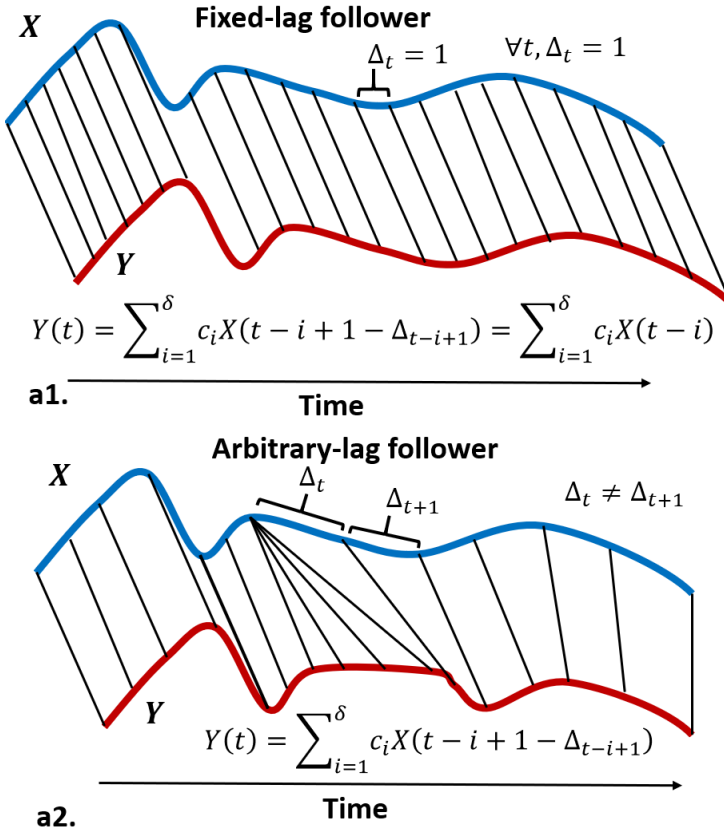


Fig. 1. (a1-2.) A leader (blue) influences a follower (red) at a specific time point via black lines. (a1.) The follower is a distorted version of a leader with a fixed lag. (a2.) The follower is a distorted version of a leader with non-fixed lags in that violates an assumption of Granger causality. Granger causality can handle only the former case and typically fails to handle later case. We propose the generalization of Granger causality to handle variable-lag situation (equation in a2.).

and do not use the results from previous paper in [5]. Moreover, we formalize *Variable-Lag Transfer Entropy* and propose a framework to infer its causal relations. We also add two new real-world datasets in this current work.

4 GRANGER CAUSALITY AND FIXED LAG LIMITATION

Let $X = (X(1), \dots, X(t), \dots)$ be a time series. We will use $X(t) \in \mathbb{R}$ to denote an element of X at time t . Given two time series X and Y , it is said that X Granger-causes [18] Y if the information of X in the past helps improve the prediction of the behavior of Y , over Y 's past information alone [6]. The typical way to operationalize this general definition of Granger causality [7] is to define it as follows:

Definition 4.1 (Granger causal relation). Let X and Y be time series, and $\delta_{max} \in \mathbb{N}$ be a maximum time lag. We define two residuals of regressions of X and Y , r_Y, r_{YX} , below:

$$r_Y(t) = Y(t) - \sum_{i=1}^{\delta_{max}} a_i Y(t-i), \quad (1)$$

$$r_{YX}(t) = Y(t) - \sum_{i=1}^{\delta_{max}} (a_i Y(t-i) + b_i X(t-i)), \quad (2)$$

where a_i and b_i are constants that optimally minimize the residual from the regression. Then X Granger-causes Y if the variance of r_{YX} is less than the variance of r_Y .

This definition assumes that, for all $t > 0$, $Y(t)$ can be predicted by the fixed linear combination of $a_1 Y(1), \dots, a_{t-\Delta} Y(t-\Delta)$ and $b_1 X(1), \dots, b_{t-\Delta} X(t-\Delta)$ with some fixed $\Delta > 0$ and every a_i, b_i is a fixed constant over time [6, 7]. However, in reality, two time series might influence each other with a sequence of arbitrary, non-fixed time lags. For example, Fig. 1(a2.) has X as a cause time series and Y as the effect time series that imitates the values of X with arbitrary lags. Because Y is not affected by X with a fixed lags and the linear combination above can change over time, the standard Granger causality tests cannot appropriately infer Granger-causal relation between X and Y even if Y is just a slightly distorted version of X with some lags. For a concrete example, consider a movement context where time series represent trajectories. Two people follow each other if they move in the same trajectory. Assuming the followers follow leaders with a fixed lag means the followers walk lockstep with the leader, which is not the natural way we walk. Imagine two people embarking on a walk. The first starts walking, the second catches up a little later. They may walk together for a bit, then the second stops to tie the shoe and catches up again. The delay between the first and the second person keeps changing, yet there is no question the first sets the course and is the cause of the second's choices where to go. Fig. 1 illustrates this example.

5 VARIABLE-LAG GRANGER CAUSALITY

Here, we propose the concept of variable-lag Granger causality, *VL-Granger causality* for short, which generalizes the Granger causal relation of Definition 4.1 in a way that addresses the fixed-lag limitation. We demonstrate the application of the new causality relation for a specific application of inferring initiators and followers of collective behavior.

Definition 5.1 (Alignment of time series). An alignment between two time series X and Y is a sequence of pairs of indices (t_i, t_j) , aligning $X(t_i)$ to $Y(t_j)$, such that for any two pairs in the alignment (t_i, t_j) and (t'_i, t'_j) , if $t_i < t'_i$ then $t_j < t'_j$ (non-crossing condition). The alignment defines a sequence of delays $P = (\Delta_1, \dots, \Delta_t, \dots)$, where $\Delta_t \in \mathbb{Z}$ and $X(t - \Delta_t)$ aligns to $Y(t)$.

Definition 5.2 (VL-Granger causal relation). Let X and Y be time series, and $\delta_{max} \in \mathbb{N}$ be a maximum time lag (this is an upper bound on the time lag between any two pairs of time series values to be considered as causal). We define residual r_{YX}^* of the regression:

$$r_{YX}^*(t) = Y(t) - \sum_{i=1}^{\delta_{max}} (a_i Y(t-i) + b_i X(t-i) + c_i X^*(t-i)). \quad (3)$$

Here $X^*(t-i) = X(t-i+1-\Delta_{t-i+1})$, where $\Delta_t > 0$ is a time delay constant in the optimal alignment sequence P^* of X and Y that minimizes the residual of the regression. The constants a_i, b_i , and c_i optimally minimize the residuals r_Y, r_{YX} , and r_{YX}^* , respectively. The terms b_i and c_i can be combined but we keep them separate to clearly denote the difference between the original

and proposed VL-Granger causality. We say that X VL-Granger-causes Y if the variance of r_{YX}^* is less than the variances of both r_Y and r_{YX} .

In order to make Definition 5.2 fully operational for this more general case (and to find the optimal constants values), we need a similarity function between two sequences which will define the optimal alignment. We propose such a similarity-based approach in Definition 5.5. Before defining this approach, we show that VL-Granger causality is the proper generalization of the traditional operational definition of Granger causality stated in Definition 4.1. Clearly, if all the delays are constant then $r_{YX}^*(t) = r_{YX}(t)$.

PROPOSITION 5.3. *Let X and Y be time series and P be their alignment sequence. If $\forall t, \Delta_t = \Delta$, then $r_{YX}^*(t) = r_{YX}(t)$.*

We must also show that the variance of $r_{YX}^*(t)$ is no greater than the variance of $r_{YX}(t)$.

PROPOSITION 5.4. *Let X and Y be time series, $P = (\Delta_1, \dots, \Delta_t, \dots)$ be their alignment sequence such that $Y(t) = X(t - \Delta_t)$. If $\exists \Delta_t, \Delta_{t'} \in P$, such that $\Delta_t \neq \Delta_{t'}$ and $\forall t, X(t) \neq X(t - 1)$, then $\text{VAR}(r_{YX}^*) < \text{VAR}(r_{YX})$.*

PROOF. Because $Y(t) = X(t - \Delta_t)$, by setting $a_i = 0, b_i = 0, c_i = 1$ for all i , we have $r_{YX}^* = 0$. In contrast, suppose $\Delta_{t+1} = \Delta_t + 1$ and $X(t - \Delta_t - 1) \neq X(t - \Delta_t) \neq X(t - \Delta_t + 1)$, so $Y(t) = Y(t + 1) = X(t - \Delta_t)$. Because a_i, b_i must be constant for all time step t to compute $r_{YX}(t)$, at time t , the regression must choose to match either 1) $Y(t) - X(t - \Delta_t) = 0$ and $Y(t + 1) - X(t + 1 - \Delta_t) \neq 0$ or 2) $Y(t) - X(t - \Delta_{t+1}) \neq 0$ and $Y(t + 1) - X(t + 1 - \Delta_{t+1}) = 0$. Both 1) and 2) options make $r_{YX}(t) + r_{YX}(t + 1) > 0$. Hence, $\text{VAR}(r_{YX}^*) < \text{VAR}(r_{YX})$. \square

According to Propositions 5.3 and 5.4, VL-Granger causality is the generalization of the Def. 4.1 and always has lower or equal variance.

Of a particular interest is the case when there is an explicit similarity relation defined over the domain of the input time series. The underlying alignment of VL-Granger causality then should incorporate that similarity measure and the methods for inferring the optimal alignment for the given similarity measure.

Definition 5.5 (Variable-lag emulation). Let \mathcal{U} be a set of time series, $X, Y \in \mathcal{U}$, and $\text{sim} : \mathcal{U} \times \mathcal{U} \rightarrow [0, 1]$ be a similarity measure between two time series.

For a threshold $\sigma \in (0, 1]$, if there exists a sequence of numbers $P = (\Delta_1, \dots, \Delta_t, \dots)$ s.t. $\text{sim}(\tilde{X}, Y) \geq \sigma$ when $\tilde{X}(t) = X(t - \Delta_t)$, then we use the following notation:

- if $\forall \Delta_t \in P, \Delta_t \geq 0$, then Y emulates X , denoted by $X \leq Y$,
- if $\forall \Delta_t \in P, \Delta_t \leq 0$, then X emulates Y , denoted by $Y \leq X$,
- if $X \leq Y$ and $Y \leq X$, then $Y \equiv X$.

We denote $X < Y$ if $X \leq Y$ and $\exists \Delta_t \in P, \Delta_t > 0$.

Note, here the sim similarity function does not have to be a distance function that obeys, among others, a triangle inequality. It can be any function that quantitatively compares the two time series. For example, it may be that when one time series increases the other decreases. We provide a more concrete and realistic example in the application setting below.

Adding this similarity measure to Definition 5.2 allows us to instantiate the notion of the optimal alignment P^* as the one that maximizes the similarity between X and Y :

$$P^* = \underset{P}{\operatorname{argmax}} \text{sim}(\tilde{X}, Y), \quad (4)$$

where $\tilde{X}(t) = X(t - \Delta_t)$ for any given P and $\Delta_t \in P$. With that addition, if $X \leq Y$, then X VL-Granger-causes Y . This allows us to operationalize VL-Granger causality by checking for variable-lag emulation, as we describe in the next section.

5.1 Example application: Initiators and followers

In this section, we demonstrate an application of the VL-Granger causal relation to finding initiators of collective behavior. The Variable-lag emulation concept corresponds to a relation of following in the leadership literature [4]. That is, $X < Y$ if Y is a *follower* of X . We are interested in the phenomenon of group convergence to a consensus behavior and answering the question of which subset of individuals, if any, initiated that collective consensus behavior. With that in mind, we now define the concept of an initiator and provide a set of subsidiary definitions that allow us to formally show (in Proposition 5.9) that initiators of collective behavior are indeed the time series that VL-Granger-cause the collective pattern in the set of the time series. In order to do this, we generalize our two-time series definitions to the case of multiple time series by defining the notion of an aggregate time series, which is consistent with previous Granger causality generalizations to multiple time series [13, 16, 39].

Definition 5.6 (Initiators). Let $\mathcal{U} = \{U_1, \dots, U_n\}$ be a set of time series. We say that $\mathcal{X} \subseteq \mathcal{U}$ is a set of initiators if $\forall U \in \mathcal{U} \setminus \mathcal{X}, \exists X \in \mathcal{X}, s.t. X < U$, and, conversely, $\forall X \in \mathcal{X} \exists U \in \mathcal{U} \setminus \mathcal{X}, s.t. X < U$. That is, every time series follows some initiator and every initiator has at least one follower.

Given a set of time series $\mathcal{U} = \{U_1, \dots, U_n\}$, and a set of time series $\mathcal{X} \subseteq \mathcal{U}$, we can define an aggregate time series as a time series of means at each step:

$$agg(\mathcal{X}) = \left(\frac{1}{|\mathcal{X}|} \sum_{U \in \mathcal{X}} U(0), \dots, \frac{1}{|\mathcal{X}|} \sum_{U \in \mathcal{X}} U(t), \dots \right) \quad (5)$$

In order to identify the state of reaching a collective consensus of a time series, while allowing for some noise, we adopt the concept of ϵ -convergence from [12].

Definition 5.7 (ϵ -convergence). Let Q and U be time series, $dist : \mathbb{R}^2 \times [0, 1]$ be a distance function, and $0 < \epsilon \leq 1/2$. If for all time $t \in [t_0, t_1]$, $dist(Q(t), U(t)) \leq \epsilon$, then Q and U ϵ -converge toward each other in the interval $[t_0, t_1]$. If $t_1 = \infty$ then we say that Q and U ϵ -converge at time t_0 .

Definition 5.8 (ϵ -convergence coordination set). Given a set of time series $\mathcal{U} = \{U_1, \dots, U_n\}$, if all time series in \mathcal{U} ϵ -converge toward $agg(\mathcal{U})$, then we say that the set \mathcal{U} is an ϵ -convergence coordination set.

We are finally ready to state the main connection between initiation of collective behavior and VL-Granger causality.

PROPOSITION 5.9. *Let $dist : \mathbb{R}^2 \times [0, 1]$ be a distance function, \mathcal{U} be a set of time series, and $\mathcal{X} \subseteq \mathcal{U}$ be a set of initiators, which is an ϵ -convergence coordination set converging towards $agg(\mathcal{X})$ in the interval $[t_0, t_1]$. For any $U, U' \in \mathcal{U}$ of length T , let*

$$\text{sim}(U, U') = \frac{\sum_t 1 - dist(U(t), U'(t))}{T}.$$

If for any $U, U' \in \mathcal{U}$ their similarity $\text{sim}(U, U') \geq 1 - \epsilon$ in the interval $[t_0, t_1]$, then $agg(\mathcal{X})$ VL-Granger-causes $agg(\mathcal{U} \setminus \mathcal{X})$ in that interval.

PROOF. Suppose $\forall X \in \mathcal{X}, X$ and $agg(\mathcal{X})$ ϵ -converge toward each other in the interval $[t_0, t_1]$, then, by definition, for all the times $t \in [t_0, t_1]$, $dist(agg(\mathcal{X})(t), X(t)) \leq \epsilon$. By the definition of

initiators, $\forall U \in \mathcal{U} \setminus X, \exists X \in X$, such that $X < U$, from some time $t_2 > t_0$. Thus, we have $\forall t$, s. t. $t_2 \leq t \leq t_1$, $\text{dist}(X(t), U(t)) \leq \epsilon$, which means $\text{dist}(\text{agg}(X), U(t)) \leq 2\epsilon$. Hence, we have $\forall t, t_2 \leq t \leq t_1$, $\text{dist}(\text{agg}(X)(t), \text{agg}(\mathcal{U} \setminus X)(t)) \leq 2\epsilon$. Since $\text{agg}(X)$ 2ϵ -converges towards some constant line v in the interval $[t_0, t_1]$ and $\text{agg}(\mathcal{U} \setminus X)(t)$ 2ϵ -converges towards the same line v in the interval $[t_2, t_1]$, hence $\text{agg}(X) < \text{agg}(\mathcal{U} \setminus X)$, which means, by definition, that $\text{agg}(X)$ VL-Granger-causes $\text{agg}(\mathcal{U} \setminus X)$. \square

We have now shown that a subset of time series are initiators of a pattern of collective behavior of an entire set if that subset VL-Granger-causes the behavior of the set. Thus, VL-Granger causality can solve the COORDINATION INITIATOR INFERENCE PROBLEM [4], which is a problem of determining whether a pattern of collective behavior was spurious or instigated by some subset of initiators and, if so, finding those initiators who initiate collective patterns that everyone follows.

6 VARIABLE-LAG TRANSFER ENTROPY CAUSALITY

Transfer Entropy has been shown to be a non-linear extension of Granger causality [9, 23]. In this section, we generalize our concept of VL-Granger causality to cover the transfer entropy concept. Given two time series X, Y , and a probability function $p(\cdot)$, the *Transfer Entropy* from X to Y can be defined below:

$$\mathcal{T}_{X \rightarrow Y} = H(Y(t) | Y_{t-1}^{(k)}) - H(Y(t) | Y_{t-1}^{(k)}, X_{t-1}^{(l)}). \quad (6)$$

Where $H(\cdot | \cdot)$ is a conditional entropy, k, l are lag constants, $Y_{t-1}^{(k)} = Y(t-1), \dots, Y(t-k)$, and $X_{t-1}^{(l)} = X(t-1), \dots, X(t-l)$. For the Shannon entropy [36], the function $H(\cdot)$ can be defined as

$$H(X) = - \sum_t p(X(t)) \log_2(p(X(t))). \quad (7)$$

The Shannon transfer entropy can be defined below [10, 23]:

$$\mathcal{T}_{X \rightarrow Y} = \sum p(Y_t^{(k)}, X_{t-1}^{(l)}) \log_2 \frac{p(Y(t) | Y_{t-1}^{(k)}, X_{t-1}^{(l)})}{p(Y(t) | Y_{t-1}^{(k)})}. \quad (8)$$

Typically, we infer whether X causes Y by comparing $\mathcal{T}_{X \rightarrow Y}$ and $\mathcal{T}_{Y \rightarrow X}$. If $\mathcal{T}_{X \rightarrow Y} > \mathcal{T}_{Y \rightarrow X}$, then X causes Y . However, the fixed-lag limitation still happens in the transfer entropy concept; in Eq. 6, we still compare $Y(t)$ with $Y_{t-1}^{(k)}$ and $X_{t-1}^{(l)}$ and no variable lags are allowed. Therefore, we formalize the *Variable-lag Transfer Entropy* or VL-Transfer entropy function as below:

$$\mathcal{T}_{X \rightarrow Y}^{\text{VL}}(P) = H(Y(t) | Y_{t-1}^{(k)}) - H(Y(t) | Y_{t-1}^{(k)}, \tilde{X}_{t-1}^{(l)}) \quad (9)$$

Where $\tilde{X}_{t-1}^{(l)} = X(t-1-\Delta_{t-1}), \dots, X(t-l-\Delta_{t-l})$ for a given P , and $\Delta_t \in P$.

PROPOSITION 6.1. *Let X and Y be time series and P be their alignment sequence. If $\forall \Delta_t \in P, \Delta_t = 0$, then $\mathcal{T}_{X \rightarrow Y}^{\text{VL}}(P) = \mathcal{T}_{X \rightarrow Y}$.*

PROOF. By setting $\Delta_t = 0$ for all t , the function $\mathcal{T}_{X \rightarrow Y}^{\text{VL}}(P)$ in Eq. 9 is equal to $\mathcal{T}_{X \rightarrow Y}$ in Eq. 6. \square

Hence, *Variable-lag Transfer Entropy* function generalizes the transfer entropy function. To find an appropriate P , we can use P^* in Eq. 4 that is a result of alignment of time series X along with Y .

7 VL-GRANGER AND TRANSFER ENTROPY CAUSALITY INFERENCE

7.1 VL-Granger Causality Inference

Given a target time series Y , a candidate causing time series X , a threshold γ , a significance level α , and the max lag δ_{max} , our framework evaluates whether X VL-Granger causes Y (with a variable lag), X Granger causes Y (with a fixed lag) or no conclusion of causation between X and Y .

In Algorithm 1 line 1-2, we have a fix-lag parameter *FixLag* that controls whether we choose to compute the normal Granger causality (*FixLag* = *true*) or VL-Granger causality (*FixLag* = *false*). We present the high level logic of the algorithm. However, the actual implementation is more efficient by removing the redundancies of the presented logic.

First, we compute Granger causality (line 1 in Algorithm 1). The flag *GrangerResult* = *true* if X Granger-causes Y , otherwise *GrangerResult* = *false*. Second, we compute VL-Granger causality (line 2 in Algorithm 1). The flag *VLGrangerResult* = *true* if X VL-Granger-causes Y , otherwise *VLGrangerResult* = *false*.

Based on the work in [7], we use the Bayesian Information Criteria (BIC) to compare the residual of regressing Y on Y past information, r_Y , with the residual of regressing Y on Y and X past information r_{YX} . We use $v_1 \ll v_2$ to represent that v_1 is less than v_2 with statistical significance by using some statistical test(s). If $BIC(r_Y) \ll BIC(r_{YX})$, then we conclude that the prediction of Y using Y, X past information is better than the prediction of Y using Y past information alone. For this work, to determine $BIC(r_Y) \ll BIC(r_{YX})$, we use *Bayesian Information Criterion difference ratio* (see Section 7.4).

After we got the results of both *GrangerResult* and *VLGrangerResult*, then we proceed to report the conclusion of causal relation between X and Y w.r.t. the following four conditions.

- **If both *GrangerResult* and *VLGrangerResult* are true**, then we compare the residual of variable-lag regression r_{DTW} with both r_Y and r_{YX} . If $BIC(r_{DTW}) < \min(BIC(r_{YX}), BIC(r_Y))$, then we conclude that X causes Y with variable lags, otherwise, X causes Y with a fix lag (line 4 in Algorithm 1).
- **If *GrangerResult* is true but *VLGrangerResult* is false**, then we conclude that X causes Y with a fix lag (line 5 in Algorithm 1).
- **If *GrangerResult* is false but *VLGrangerResult* is true**, then we conclude that X causes Y with variable lags (line 6 in Algorithm 1).
- **If both *GrangerResult* and *VLGrangerResult* are false**, then we cannot conclude whether X causes Y (line 7 in Algorithm 1).

Note that we assume the maximum lag value δ_{max} is given as an input, as it is for all definitions of Granger causality. For practical purposes, a value of a large fraction (e.g., half) of the length of the time series can be used. However, there is, of course, a computational trade-off between the magnitude of δ_{max} and the time it takes to compute Granger causality by almost all methods.

In the next section, we describe the details of VL-Granger function that we use in Algorithm 1: line 1-2.

7.2 VL-Granger causality operationalization

Given time series X, Y , a threshold γ , a significance level α , the maximum possible lag δ_{max} , and whether we want to check for variable or fixed lag *FixLag*, Algorithm 2 reports whether X causes Y by setting *GrangerResult* to true or false, and by reporting on two residuals r_Y and r_{YX} .

First, we compute the residual r_Y of regressing of Y on Y 's information in the past (line 1). Then, we regress $Y(t)$ on Y and X past information to compute the residual r_{YX} (line 2). If $BIC(r_{YX}) \ll BIC(r_Y)$, then X Granger-causes Y and we set *GrangerResult* = *true* (line 7). If *FixLag* is true, then we report the result of typical Granger causality. Otherwise, we consider

Algorithm 1: Time-lag test function

```

input :  $X, Y, \sigma, \alpha, \delta_{max}$ 
output:  $XGrangerCausesY$ 
1 ( $GrangerResult, r_Y, r_{YX}$ ) =  $VLGrangerFunc(X, Y, \sigma, \alpha, \delta_{max}, FixLag = true)$ ;
2 ( $VLGrangerResult, r_Y, r_{DTW}$ ) =  $VLGrangerFunc(X, Y, \sigma, \alpha, \delta_{max}, FixLag = false)$ ;
3 if  $GrangerResult = true$  then
4   | if  $VLGrangerResult = true$  then
5     | if  $BIC(r_{DTW}) \ll \min(BIC(r_{YX}), BIC(r_Y))$  then
6       |  $XGrangerCausesY = \text{TRUE-VARIABLE}$ ;
7     | else
8       |  $XGrangerCausesY = \text{TRUE-FIXED}$ ;
9     | end
10    | else
11    |  $XGrangerCausesY = \text{TRUE-FIXED}$ ;
12    | end
13  | else
14  | if  $VLGrangerResult = true$  then
15    |  $XGrangerCausesY = \text{TRUE-VARIABLE}$ ;
16  | else
17    |  $XGrangerCausesY = \text{NONE}$ ;
18  | end
19 end
20 return  $XGrangerCausesY$ ;

```

VL-Granger causality (lines 3-5) by computing the emulation relation between X^{DTW} and Y where X^{DTW} is a version of X that is reconstructed through DTW and is most similar to Y , captured by $DTWReconstructionFunction(X, Y)$ which we explain in Section 7.3.

Afterwards, we do the regression of Y on X^{DTW} 's past information to compute residual r_{DTW} (line 4). Finally, we check whether $BIC(r_{DTW}) \ll BIC(r_Y)$ (line 6-9) (see Section 7.4). If so, X VL-Granger-cause Y . In the next section, we describe the details of how to construct X^{DTW} and how to estimate the emulation similarity value $simValue$.

7.3 Dynamic Time Warping for inferring VL-Granger causality.

In this work, we propose to use Dynamic Time Warping (DTW) [31], which is a standard distance measure between two time series. DTW calculates the distance between two time series by aligning sufficiently similar patterns between two time series, while allowing for local stretching (see Figure 1). Thus, it is particularly well suited for calculating the variable lag alignment.

Given time series X and Y , Algorithm 3 reports reconstructed time series X^{DTW} based on X that is most similar to Y , as well as the emulation similarity $simValue$ between the two series. First, we use $DTW(X, Y)$ to find the optimal alignment sequence $\hat{P} = (\Delta_1, \dots, \Delta_t, \dots)$ between X and Y , as defined in Definition 5.1. Efficient algorithms for computing $DTW(X, Y)$ exist and they can incorporate various kernels between points [26, 31]. Then, we use \hat{P} to construct X^{DTW} where $X^{DTW}(t) = X(t - \Delta_t)$. However, we also use cross-correlation to normalize Δ_t since DTW is sensitive to a noise of alignment (Algorithm 3 line 3-5).

Afterwards, we use X^{DTW} to predict Y instead of using only X information in the past in order to infer a VL-Granger causal relation in Definition 5.2. The benefit of using DTW is that it can

Algorithm 2: VLGrangerFunc

```

input :  $X, Y, \delta_{max}, \alpha, \gamma, FixLag$ 
output:  $GrangerResult, r_Y, r_{YX}$ 
1 Regress  $Y(t)$  on  $Y(t - \delta_{max}), \dots, Y(t - 1)$ , then compute the residual  $r_Y(t)$ ;
if  $FixLag$  is true then
2 | Regress  $Y(t)$  on  $Y(t - \delta_{max}), \dots, Y(t - 1)$  and  $X(t - \delta_{max}), \dots, X(t - 1)$ , then compute the
   | residual  $r_{YX}(t)$ ;
else
3 |  $X^{DTW}, simValue = DTWReconstructionFunction(X, Y)$  ;
4 | Regress  $Y(t)$  on  $Y(t - \delta_{max}), \dots, Y(t - 1)$  and  $X^{DTW}(t - \delta_{max}), \dots, X^{DTW}(t - 1)$ , then
   | compute the residual  $r_{DTW}$ ;
5 |  $r_{YX} = r_{DTW}$ ;
end
6 if  $BIC_1(r_{YX}) \ll BIC_0(r_Y)$  then
7 |  $GrangerResult = true$ 
8 else
9 |  $GrangerResult = false$  ;
end
10 return  $GrangerResult, r_Y, r_{YX}$ ;

```

match time points of Y and X with non-fixed lags (see Figure 1). Let $\hat{P} = (\Delta_1, \dots, \Delta_t, \dots)$ be the DTW optimal warping path of X, Y such that for any $\Delta_t \in \hat{P}$, $Y(t)$ is most similar to $X(t - \Delta_t)$.

In addition to finding X^{DTW} , $DTWReconstructionFunction$ estimates the emulation similarity $simValue$ between X, Y in line 3. For that, we adopt the measure from [4] below:

$$s(\hat{P}) = \frac{\sum_{\Delta_t \in \hat{P}} \text{sign}(\Delta_t)}{|\hat{P}|}, \quad (10)$$

where $0 < s(\hat{P}) \leq 1$ if $X \leq Y$, $-1 \leq s(\hat{P}) < 0$ if $Y \leq X$, otherwise zero. Since the $\text{sign}(\Delta_t)$ represents whether Y is similar to X in the past ($\text{sign}(\Delta_t) > 0$) or X is similar to Y in the past ($\text{sign}(\Delta_t) < 0$), by comparing the sign of $\text{sign}(\Delta_t)$, we can infer whether Y emulates X . The function $s(\hat{P})$ computes the average sign of $\text{sign}(\Delta_t)$ for the entire time series. If $s(\hat{P})$ is positive, then, on average, the number of times that Y is similar to X in the past is greater than the number of times that X is similar to some values of Y in the past. Hence, $s(\hat{P})$ can be used as a proxy to determine whether Y emulates X or vice versa. We use *dtw* R package [17] for our DTW function.

7.4 Bayesian Information Criterion difference ratio for VL-Granger causality

Given $RRSS$ is a restricted residual sum of squares from a regression of Y on Y past, and T is a length of time series, the BIC of null model can be defined below.

$$BIC_0(r_Y) = \frac{RRSS(r_Y)}{T} T^{(\delta_{max}+1)/T}, \quad (11)$$

For unrestricted model, given $URSS$ is an unrestricted residual sum of squares from a regression of Y on Y, X past, and T is a length of time series, the BIC of alternative model can be defined below.

$$BIC_1(r_{YX}) = \frac{URSS(r_{YX})}{T} T^{(2\delta_{max}+1)/T}, \quad (12)$$

Algorithm 3: DTWReconstructionFunction

```

input :  $X, Y$ 
output:  $X^{DTW}, simValue$ 
1  $\hat{P} = (\Delta_1, \dots, \Delta_t, \dots) = DTW(X, Y)$ ;
2  $\hat{P}_0 = (\Delta_0, \dots, \Delta_0, \dots) = CrossCorrelation(X, Y)$ ;
3 for all  $t$  do
4   if  $DIST(X(t - \Delta_t), Y(t)) < DIST(X(t - \Delta_0), Y(t))$  then
5     | set  $X^{DTW}(t - 1) = X(t - \Delta_t)$  and  $\hat{P}^*(t) = \Delta_t$ ;
   else
6     | set  $X^{DTW}(t - 1) = X(t - \Delta_0)$  and  $\hat{P}^*(t) = \Delta_0$ ;
   end
end
7  $simValue = s(\hat{P}^*)$ ;
   Return  $X^{DTW}, simValue$ ;

```

We use the *Bayesian Information Criterion difference ratio* as a main criteria to determine whether X Granger-causes Y or determining $BIC_1(r_{YX}) \ll BIC_0(r_Y)$ in Algorithm 2 line 6, which can be defined below:

$$r(BIC_0(r_Y), BIC_1(r_{YX})) = \frac{BIC_0(r_Y) - BIC_1(r_{YX})}{BIC_0(r_Y)}. \quad (13)$$

The ratio $r(\cdot, \cdot)$ is within $[-\infty, 1]$. The closer $r(\cdot, \cdot)$ to 1, the better the performance of alternative model is compared to the null model. We can set the threshold $\gamma \in [0, 1]$ to determine whether X Granger-causes Y , i.e. $r(BIC_0(r_Y), BIC_1(r_{YX})) \geq \gamma$ implies X Granger-causes Y . Other options of determining X Granger-causes Y is to use F-test or the emulation similarity *simValue*.

7.5 VL-Transfer-Entropy Causality Inference

Given a target time series Y , a candidate causing time series X , and the max lag δ_{max} , our framework evaluates whether X VL-Transfer-Entropy causes Y (with a variable lag), X Transfer-Entropy-causes Y (with a fixed lag) or no conclusion of causation between X and Y .

In Algorithm 4 line 1-2, we have a fix-lag parameter *FixLag* that controls whether we choose to compute the normal Transfer-Entropy causality (*FixLag = true*) or VL-Transfer-Entropy causality (*FixLag = false*).

First, we compute Transfer Entropy causality (line 1 in Algorithm 4). The flag *TransEResult = true* if X Transfer-Entropy-causes Y , otherwise *TransEResult = false*. Second, we compute VL-Transfer-Entropy causality (line 2 in Algorithm 4). The flag *VLTransEResult = true* if X VL-Transfer-Entropy-causes Y , otherwise *VLTransEResult = false*.

To determine whether X Transfer-Entropy-causes Y , we can use the *Transfer Entropy Ratio*.

$$\mathcal{T}(X, Y)_{ratio} = \frac{\mathcal{T}_{X \rightarrow Y}}{\mathcal{T}_{Y \rightarrow X}}. \quad (14)$$

The *VL-Transfer Entropy Ratio* is defined below:

$$\mathcal{T}^{VL}(X, Y)_{ratio} = \frac{\mathcal{T}_{X \rightarrow Y}^{VL}}{\mathcal{T}_{Y \rightarrow X}^{VL}}. \quad (15)$$

The value $\mathcal{T}(X, Y)_{ratio}$ is greater than one implies that X Transfer-Entropy-causes Y . The higher $\mathcal{T}(X, Y)_{ratio}$ implies the higher strength of X causes Y . The same is true for $\mathcal{T}^{VL}(X, Y)_{ratio}$.

Algorithm 4: Transfer Entropy Time-lag test function

```

input :  $X, Y, \delta_{max}$ 
output:  $XTransferEntropyCausesY$ 
1 ( $TransEResult, \mathcal{T}_{X \rightarrow Y}, \mathcal{T}_{Y \rightarrow X}$ ) = VLTransferEFunc( $X, Y, \sigma, \alpha, \delta_{max}, FixLag = true$ );
2 ( $VLTransEResult, \mathcal{T}_{X \rightarrow Y}^{VL}, \mathcal{T}_{Y \rightarrow X}^{VL}$ ) = VLTransferEFunc( $Y, X, \sigma, \alpha, \delta_{max}, FixLag = false$ );
3 if  $TransEResult = true$  then
  | if  $VLTransEResult = true$  then
4   | if  $\mathcal{T}(X, Y)_{ratio} < \mathcal{T}^{VL}(X, Y)_{ratio}$  then
  |   |  $XTransferEntropyCausesY = TRUE-VARIABLE$ ;
  |   else
  |     |  $XTransferEntropyCausesY = TRUE-FIXED$ ;
  |   end
  | else
5   |  $XTransferEntropyCausesY = TRUE-FIXED$ ;
  | end
  else
6   | if  $VLTransEResult = true$  then
  |   |  $XTransferEntropyCausesY = TRUE-VARIABLE$ ;
  |   else
7   | |  $XTransferEntropyCausesY = NONE$ ;
  |   end
  end
8 return  $XTransferEntropyCausesY$ ;

```

After we got the results of both $TransEResult$ and $VLTransEResult$, then we proceed to report the conclusion of causal relation between X and Y w.r.t. the following four conditions.

- **If both $TransEResult$ and $VLTransEResult$ are true**, then we compare the $\mathcal{T}(X, Y)_{ratio}$ with $\mathcal{T}^{VL}(X, Y)_{ratio}$. If $\mathcal{T}(X, Y)_{ratio} < \mathcal{T}^{VL}(X, Y)_{ratio}$, then we conclude that X causes Y with variable lags, otherwise, X causes Y with a fix lag (line 4 in Algorithm 4).
- **If $TransEResult$ is true but $VLTransEResult$ is false**, then we conclude that X causes Y with a fix lag (line 5 in Algorithm 4).
- **If $TransEResult$ is false but $VLTransEResult$ is true**, then we conclude that X causes Y with variable lags (line 6 in Algorithm 4).
- **If both $TransEResult$ and $VLTransEResult$ are false**, then we cannot conclude whether X causes Y (line 7 in Algorithm 4).

7.6 VL-Transfer-Entropy causality operationalization

Given time series X, Y , and the maximum possible lag δ_{max} , and whether we want to check for variable or fixed lag $FixLag$, Algorithm 5 reports whether X causes Y by setting $TransEResult$ to true or false, and by reporting on two transfer entropy values: $\mathcal{T}_{X \rightarrow Y}$ and $\mathcal{T}_{Y \rightarrow X}$.

First, if $FixLag$ is true, then we compute the transfer entropy (line 1) using $RTransferEntropy(X, Y)$ [10]. If $FixLag$ is false, then, we reconstructed X^{DTW} using $DTWReconstructionFunction(X, Y)$ in Section 7.3 (line 2). We compute the VL-transfer entropy (line 3) using $RTransferEntropy(X^{DTW}, Y)$.

If the ratio $\mathcal{T}(X, Y)_{ratio} > 1$, then X causes Y and we set $TransEResult = true$ (line 5), otherwise, $TransEResult = false$ (line 7).

Algorithm 5: VLTransferEFunc

```

input :  $X, Y, \delta_{max}, FixLag$ 
output:  $TransEResult, \mathcal{T}_{X \rightarrow Y}, \mathcal{T}_{Y \rightarrow X}$ 
if  $FixLag$  is true then
1 |  $\mathcal{T}_{X \rightarrow Y}, \mathcal{T}_{Y \rightarrow X} = RTransferEntropy(X, Y)$  [10];
else
2 |  $X^{DTW}, simValue = DTWReconstructionFunction(X, Y)$ ;
3 |  $\mathcal{T}_{X \rightarrow Y}, \mathcal{T}_{Y \rightarrow X} = RTransferEntropy(X^{DTW}, Y)$  [10];
end
4 if  $\mathcal{T}(X, Y)_{ratio} > 1$  then
5 |  $TransEResult = true$ 
6 else
7 |  $TransEResult = false$ ;
end
8 return  $TransEResult, \mathcal{T}_{X \rightarrow Y}, \mathcal{T}_{Y \rightarrow X}$ ;

```

Table 1. Notations and symbols

Term and notation	Description
T	Length of time series.
γ	Threshold of BIC difference ratio in Section 7.4.
δ_{max}	Parameter of the maximum length of time delay
BIC	Bayesian Information Criterion, which is used as a proxy to compare the residuals of regressions of two time series.
$A < B$	B emulates A .
\mathcal{N}	Normal distribution.
ARMA or A.	Auto-Regressive Moving Average model.
VL-G	Variable-lag Granger causality with BIC difference ratio: X causes Y if BIC difference ratio $r(BIC_0(r_Y), BIC_1(r_{YX})) \geq \gamma$.
G	Granger causality [7]
CG	Copula-Granger method [24]
SIC	Spectral Independence Criterion method [35]
TE	Transfer entropy [10]
VL-TE	Variable-lag transfer entropy

8 EXPERIMENTS

We measured our framework performance on the task of inferring causal relations using both simulated and real-world datasets. The notations and symbols we use in this section are in Table 1.

8.1 Experimental setup

We tested the performance of our method on synthetic datasets, where we explicitly embedded a variable-lag causal relation, as well as on biological datasets in the context of the application of identifying initiators of collective behavior, and on other two real-world casual datasets.

We compared our methods, VL-Granger causality (VL-G) and VL-Transfer entropy (VL-TE), with several existing methods: Granger causality with F-test (G) [7], Copula-Granger method (CG) [24], Spectral Independence Criterion method (SIC) [35], and transfer entropy (TE) [10].

In this paper, we explore the choice of δ_{max} in $\{0.1T, 0.2T, 0.3T, 0.4T\}$ for all methods to analyze the sensitivity of each method, where T is the length of time series, and set $\gamma = 0.5$ as default unless explicitly stated otherwise.

8.2 Datasets

8.2.1 Synthetic data: pairwise level. The main purpose of the synthetic data is to generate settings that explicitly illustrate the difference between the original Granger causality, transfer entropy methods and the proposed variable-lag approaches. We generated pairs of time series for which the fixed-lag causality methods would fail to find a relationship but the variable-lag approach would find the intended relationships.

We generated a set of synthetic time series of 200 time steps. We generated two sets of pairs of time series X and Y . First, we generated X either by drawing the value of each time step from a normal distribution with zero mean and a constant variance ($X(t) \sim \mathcal{N}$) or by Auto-Regressive Moving Average model (ARMA or A.) with $X(t) = 0.9\mu + 0.1X(t-1)$.

The first set we generated was of explicitly related pairs of time series X and Y , where Y emulates X with some time lag $\Delta \in [1, 20]$ ($X < Y$). One way to ensure lag variability is to “turn off” the emulation for some time. For example, Y remains constant between 110th and 150th time steps. This makes Y a variable-lag follower of X . Figure 3 shows examples of the generated time series.

The second set of time series pairs X and Y were generated independently and as a result have no causal relation. We used these pairs to ensure that our method does not infer spurious relations.

We set the significance level for both F-test and independence test at $\alpha = 0.01$. We considered there to be a causal relation only if $r(BIC_0(r_Y), BIC_1(r_{YX})) \geq \gamma$ for our method.

8.2.2 Synthetic data: group level. This experiment explores the ability of causal inference methods to retrieve *multiple* causes of a time series Y_{ij} , which is generated from multiple time series X_i, X_j . Fig. 2 shows the ground truth causal graph we used to generate simulated datasets. The edges represent causal directions from the cause time series (e.g. X_1) to the effect time series (e.g. Y_1). Y_{ij} represents the time series generated by $agg(\{X'_i, X'_j\})$, where $X_i < X'_i$ and $X_j < X'_j$ with some fixed lag $\Delta \in [1, 20]$. The task is to infer edges of this causal graph from the time series. We generated time series for each generator model 100 times. We set $\gamma = 0.03$ in this experiment due to the weak signal of X causes Y when there are multiple causes of Y . There are also two generators for X_1, X_2, X_3 : normal distribution and ARMA model.

8.2.3 Schools of fish. We used the dataset of golden shiners (*Notemigonus crysoleucas*) that is publicly available. The dataset has been collected for the study of information propagation over the visual fields of fish [42]. A coordination event consists of two-dimensional time series of fish movement that are recorded by video. The time series of fish movement are around 600 time steps. The number of fish in each dataset is around 70 individuals, of which 10 individuals are “informed” fish who have been trained to go to a feeding site. Trained fish lead the group to feeding sites while the rest of the fish just follow the group. We represent the dataset as a pair of aggregated time series: X being the aggregated time series of the directions of trained fish and Y being the aggregated time series of the directions of untrained fish (see Fig. 4). The task is to infer whether X (trained fish) is a cause of Y (the rest of the group).

8.2.4 Troop of baboons. We used another publicly available dataset of animal behavior, the movement of a troop of olive baboons (*Papio anubis*). The dataset consists of GPS tracking information from 26 members of a troop, recorded at 1 Hz from 6 AM to 6 PM between August 01, 2012 and August 10, 2012. The troop lives in the wild at the Mpala Research Centre, Kenya [14, 43]. For the analysis, we selected the 16 members of the troop that have GPS information available for 10

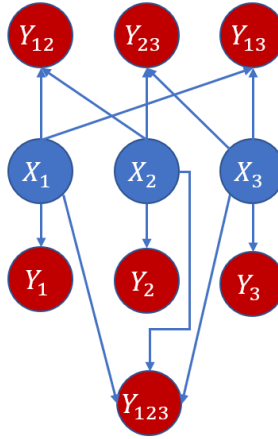


Fig. 2. The causal graph where the edges represent causal directions from the cause time series (e.g. X_1) to the effect time series (e.g. Y_1). Y_{ij} represents a time series generated by $agg(\{X'_i, X'_j\})$, where $X_i < X'_i$ with some fixed lag Δ .

Table 2. Running time of our approaches with varying time series length T and maximum time delay δ_{max} .

δ_{max}/T	Running time (sec)			
	VL-G		VL-TE	
	$T = 5000$	$T = 20000$	$T = 5000$	$T = 20000$
0.05	5.39	110.00	17.57	126.02
0.10	7.90	128.19	17.42	121.38
0.20	9.22	200.17	17.93	131.23

consecutive days, with no missing data. We selected a set of trajectories of lat-long coordinates from a highly coordinated event that has the length of 600 time steps (seconds) for each baboon. This known coordination event is on August 02, 2012 in the morning, with the baboon ID3 initiating the movement, followed by the rest of the troop [4]. Again, the goal is to infer ID3 (time series X) as the cause of the movement of the rest of the group (aggregate time series Y) (see Fig. 5).

8.2.5 Gas furnace. This dataset consists of information regarding a gas consumption by a gas furnace [11]. X is time series of gas consumption rate and Y is time series of CO_2 rate produced by a gas furnace (see Fig. 6). Both X, Y have 296 time steps.

8.2.6 Old Faithful geyser eruption. This dataset consists of information regarding eruption durations and intervals between eruption events at Old Faithful geyser [8]. X is time series of eruption duration and Y is time series of the interval between current eruption and the next eruption (see Fig. 7). Both X, Y have 298 time steps.

8.3 Time complexity and running time

The main cost of computation in our approach is DTW. We used the ‘‘Windowing technique’’ for the search area of warping [22]. The main parameter for windowing technique is the maximum time delay δ_{max} . Hence, the time complexity of VL-G is $O(T\delta_{max})$. The time complexity of TE can be at most $O(T^3)$ [37], which makes VL-TE has the same time complexity. Table 2 shows the running

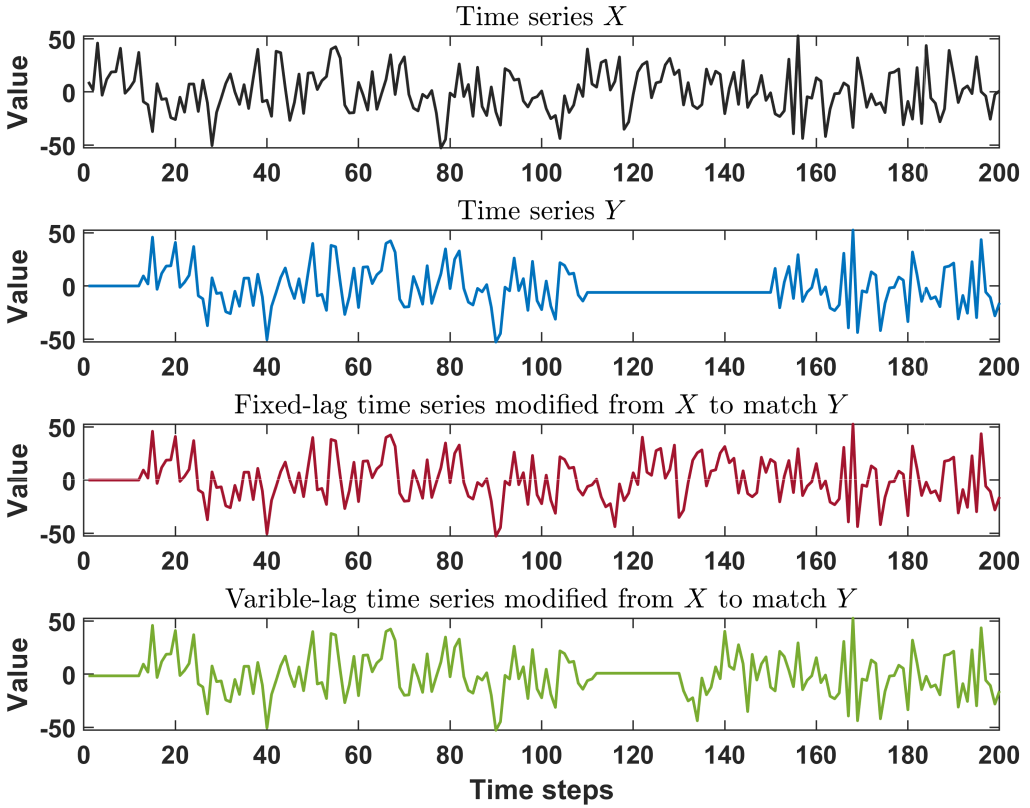


Fig. 3. The comparison between the original time series X , variable-lag follower Y , fixed-lag time series modified from X to match Y , and variable-lag time series modified from X to match Y . The traditional Granger causality uses only fixed-lag version of X to infer whether X causes Y , while our approach uses both versions of X to determine the causality between X, Y . Both X, Y are generated from \mathcal{N} . Y remains constant from time 110 to 150, which makes it a variable-lag follower of X .

time of our approach on time series with the varying length ($T \in \{5000, 20000\}$) and maximum time delay ($\delta_{max} \in \{0.05T, 0.1T, 0, 2T\}$).

9 RESULTS

We report the results of our proposed approaches and other methods on both synthetic and real-world datasets. We also explore how the performance of the methods depends on the basic parameter, δ_{max} .

9.1 Synthetic data: pairwise level

Table 3 (1st-5th rows) shows the results of the accuracy of inferring causal relations and directions. For each row, we repeated the experiment 100 times on simulated datasets and computed the accuracy and reported the mean. The result shows that our methods, VL-G, performed better than the rest of other methods. VL-TE also performed better than TE. Moreover, we also investigate the sensitivity of varying the value of the δ_{max} parameter for all methods. We aggregated the accuracy

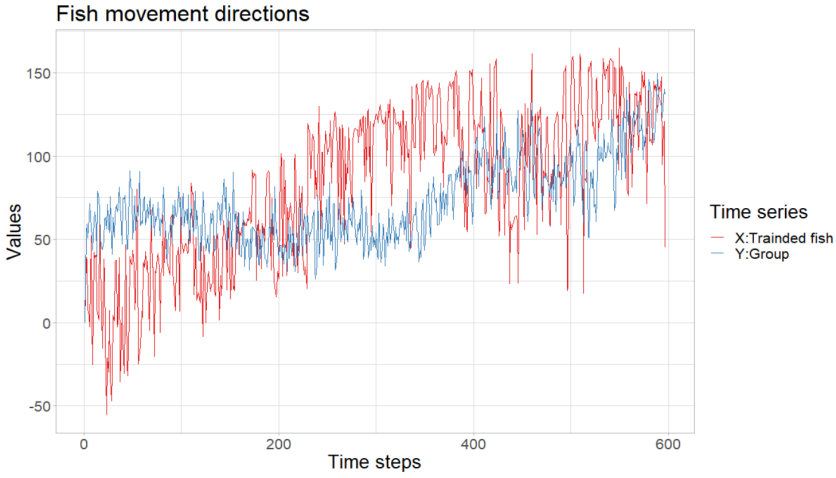


Fig. 4. Time series of fish movement: X is an aggregated time series of movement directions of trained fish and Y is an aggregated time series of movement directions of untrained fish, which is the rest of the group.

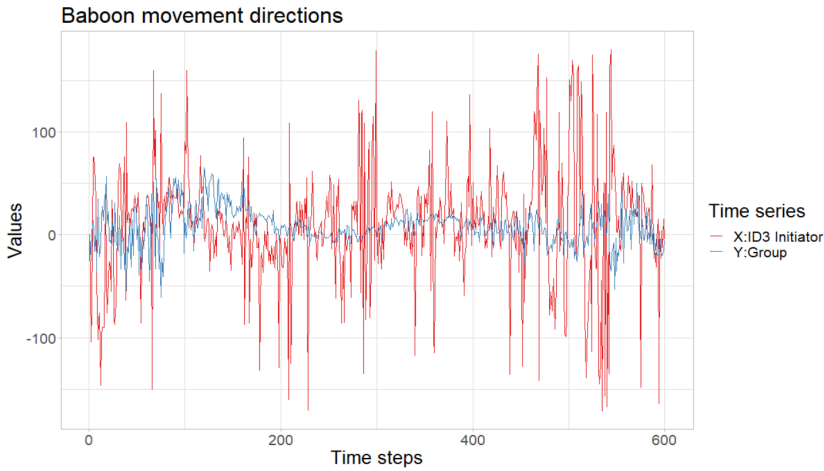


Fig. 5. Time series of baboon movement: X is a time series of movement directions of ID3 and Y is an aggregated time series of movement directions of the rest of the group.

Table 3. Average accuracy of inferring causal direction from various cases. Each column represents a method. Each row represents a model. “ $\mathcal{N}:X$ ” means X was generated from a normal distribution and “ $\mathcal{A}:X$ ” means X was generated from ARMA model. $X < Y$ means X causes Y by an emulation relation and $X \not< Y$ means no causal relation. We varied δ_{max} from 10% to 40% of time series length T and reported the average.

	VL-G	G	CG	SIC	TE	VL-TE
$\mathcal{N}:X < Y$	1.00	1.00	0.79	0.64	0.72	0.93
$\mathcal{N}:X \not< Y$	0.99	0.88	0.67	0.34	0.52	0.68
$\mathcal{A}:X < Y$	0.99	1.00	0.79	0.68	0.84	0.92
$\mathcal{A}:X \not< Y$	0.99	0.66	0.50	0.30	0.50	0.76
$\mathcal{N}:X, \mathcal{A}:Y$	0.99	0.91	0.75	0.57	0.50	0.76

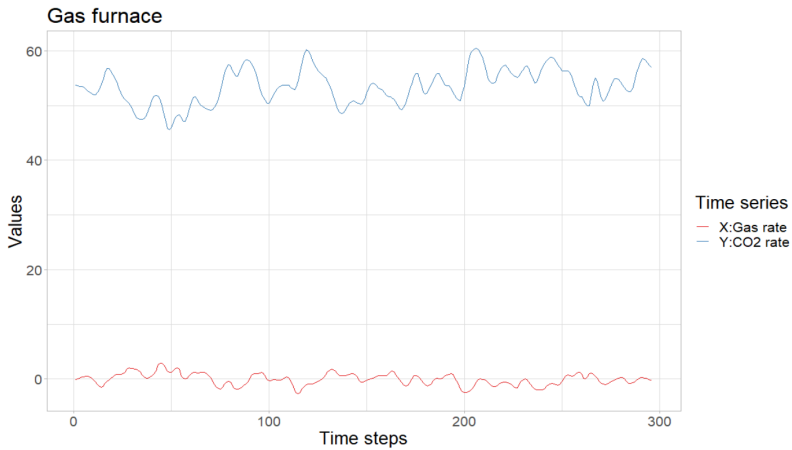


Fig. 6. Time series of Gas furnace: X is time series of gas consumption rate and Y is time series of CO_2 .

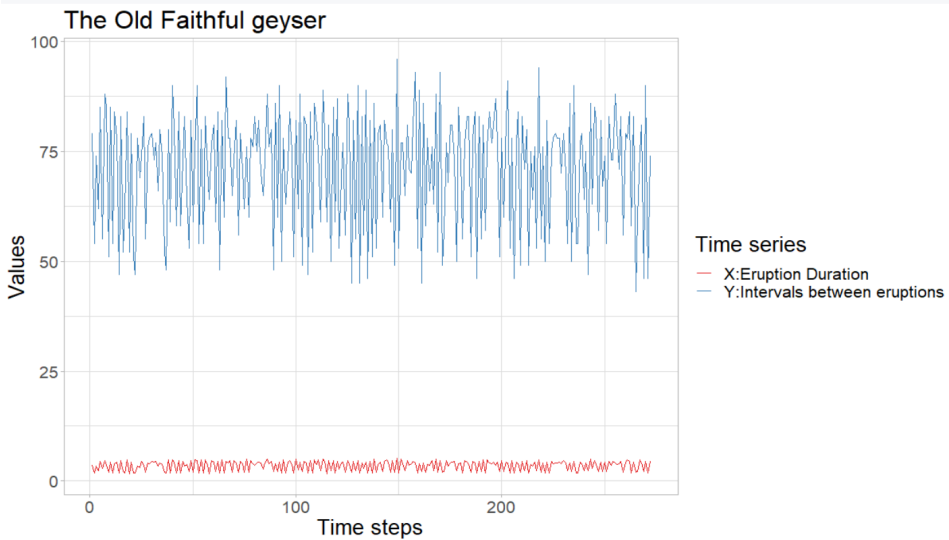


Fig. 7. Time series of the Old Faithful geyser eruption: X is time series of eruption duration and Y is time series of the interval between current eruption and the next eruption.

of inferring causal direction from various cases that have the same δ_{max} value and report the result. The result in Fig. 8 shows that our approaches: VL-G, can maintain the high accuracy throughout the range of the values of δ_{max} .

9.2 Synthetic data: group level

Table 4 shows the result of causal graph inference. The VL-G performed the best overall with the highest F1 score. This result reflects the fact that our approaches can handle complicated time series in causal inference task better than the rest of other methods. VL-TE also performed better than VL-TE. In addition, we aggregated $X = agg(\{X_1, X_2, X_3\})$ and the rest of time series

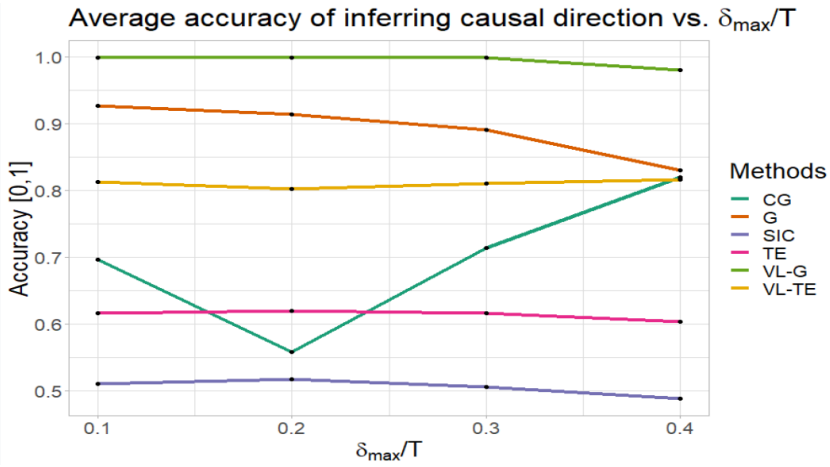


Fig. 8. Average accuracy of inferring causal direction as a function of δ_{max} . x -axis represents the value of δ_{max} as a fraction of the time series length T and y -axis is the average accuracy.

Table 4. The results of the precision, recall, and F1-score values of edges inference of causal graph in Fig. 2. Each row is a method and each column is a measure type. We varied δ_{max} from 10% to 40% of time series length T and reported the average.

Methods	Causal graph			Group: $X < Y$
	Precision	Recall	F1 score	Accuracy
VL-G	0.88	0.91	0.89	1.00
G	0.63	0.84	0.69	1.00
CG	0.41	0.64	0.47	0.13
SIC	0.16	0.60	0.25	0.33
TE	0.21	0.79	0.34	1.00
VL-TE	0.26	0.79	0.39	1.00

Table 5. The result of inferring causal relations in real-world datasets. Each row is a dataset and each column is a method. An element is one if a method successfully inferred a causal relation with some parameter, while an element is zero if no parameter setting in a method can be used to successfully infer a causal relation.

Case	VL-G	G	CG	SIC	TE	VL-TE
Fish	1	0	1	0	1	1
Baboon	1	1	1	1	1	1
Gas furnace	1*	1	0	1	1	1
Old faithful geyser	1*	0	1	1	0	1

$Y = agg(\{Y_1, Y_2, \dots, Y_{123}\})$, then we measured the ability of methods to infer that X is a cause of Y . The results, which are in the “Group: $X < Y$ ” column in Table 4, show that VL-G, G, TE and VL-TE performed well in this task, while CG and SIC failed to infer causal relations.

9.3 Real-world datasets

Table 5 shows results of inferring causal relations in real-world datasets. For VL-G, it performed better than G. However, BIC difference ratio failed to infer causal relations of gas furnace and old

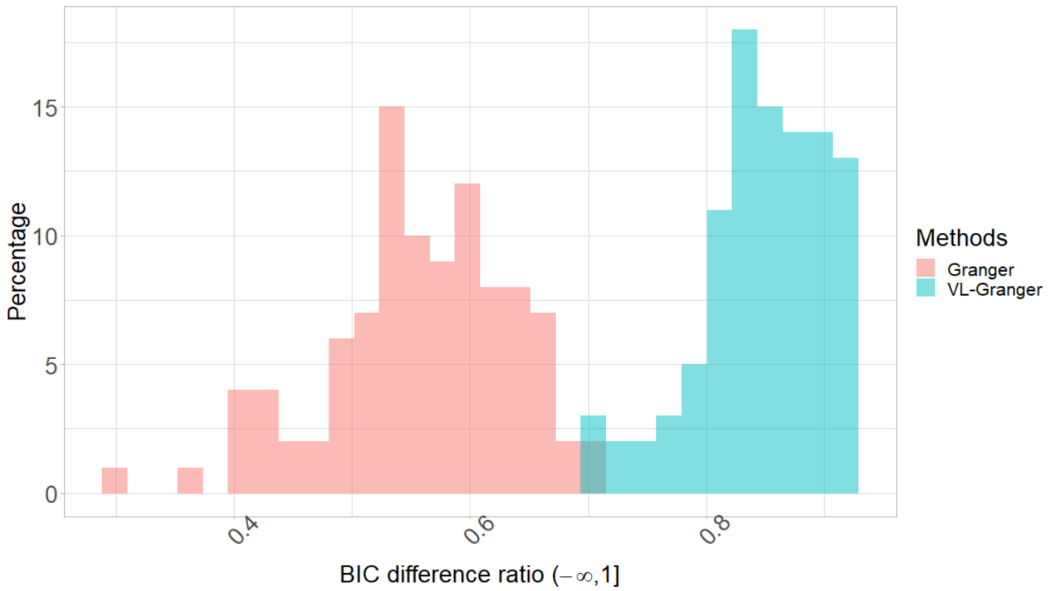


Fig. 9. Empirical distributions of BIC difference ratios of VL-Granger and Granger methods inferred from simulation data of $X < Y$. Higher BIC difference ratio implies better model if X is the cause of Y .

faithful geyser datasets but F-test successfully inferred causal relations in all datasets. Typically, a causal relation that has a high BIC difference ratio can also be detected to have a causal relation by F-test but not vice versa. This suggests that gas furnace and old faithful geyser have weak causal relations. For G, the method cannot detect fish and Old faithful geyser datasets. This suggests that both datasets have a high-level of variable lags that a fixed-lag assumption in G has an issue. For CG, SIC, and TE, they failed in one dataset each. This implies that some dataset that a specific approach failed to detect a causal relation has broke some assumption of a specific approach. Lastly, VL-TE was able to detect all causal relations.

For the old faithful geyser dataset, both G and TE failed to detect a causal relation while both VL-G and VL-TE successfully inferred a causal relation. This implies that this dataset has a high-level of variable lags that broke a fix-lag assumption of G and TE.

9.4 Variable lags vs. fixed lag

9.4.1 VL-Granger causality. To compare the performance of VL-G and G, we simulated 100 datasets of $X < Y$ with variable lags. Since $X < Y$, a higher BIC difference ratio implies a better result. Fig. 9 shows the results of BIC difference ratio for VL-G and G. Obviously, VL-G has a higher BIC difference ratio than G's. This suggests that VL-G was able to capture stronger signal of X causes Y .

9.4.2 VL-Transfer Entropy. To compare the performance of VL-TE and TE, we also simulated 100 datasets of $X < Y$ with variable lags. Since $X < Y$, a higher transfer entropy ratio implies a better result. Fig. 10 shows the results of transfer entropy ratio for VL-TE and TE. Obviously, VL-TE has a higher transfer entropy ratio than TE's. This suggests that VL-TE was able to capture stronger signal of X causes Y .

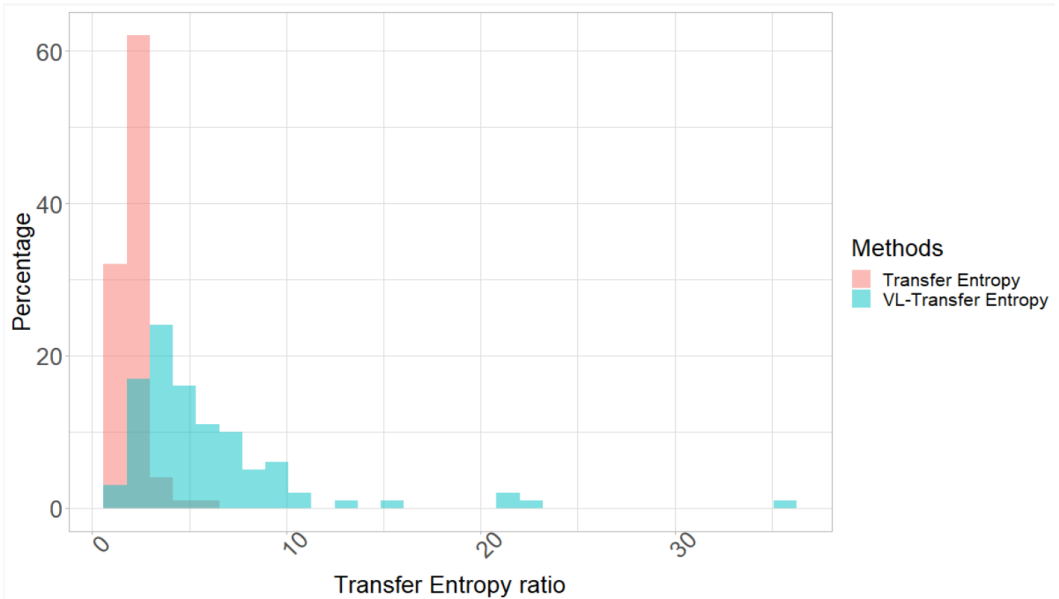


Fig. 10. Empirical distributions of transfer entropy ratios of VL-transfer entropy and transfer entropy methods inferred from simulation data of $X < Y$. Higher transfer entropy ratio implies better model if X is the cause of Y .

10 CONCLUSIONS

In this work, we proposed a method to infer Granger and transfer entropy causal relations in time series where the causes influence effects with arbitrary time delays, which can change dynamically. We formalized a new Granger causal relation and a new transfer entropy causal relation, proving that they are true generalizations of the traditional Granger causality and transfer entropy respectively. We demonstrated on both carefully designed synthetic datasets and noisy real-world datasets that the new causal relations can address the arbitrary-time-lag influence between cause and effect, while the traditional Granger causality and transfer entropy cannot. Moreover, in addition to improving and extending Granger causality and transfer entropy, our approach can be applied to infer leader-follower relations, as well as the dependency property between cause and effect. We have shown that, in many situations, the causal relations between time series do not have a lock-step connection of a fixed lag that the traditional Granger causality and transfer entropy assume. Hence, traditional Granger causality and transfer entropy missed true existing causal relations in such cases, while our methods correctly inferred them. Our approach can be applied in any domain of study where the causal relations between time series is of interest. The R package entitled *VLTimeSeriesCausality* is provided at [3].

REFERENCES

- [1] [n. d.]. Granger Causality Package in MATLAB. <https://www.mathworks.com/matlabcentral/fileexchange/25467-granger-causality-test>.
- [2] [n. d.]. Granger Causality Package in R. <https://www.rdocumentation.org/packages/MSBVAR/versions/0.9-2/topics/granger.test>.
- [3] Chainarong Amornbunchornvej. [n. d.]. *VLTimeSeriesCausality*: R package for variable-lag causal inference in time series. <https://github.com/DarkEyes/VLTimeSeriesCausality>. Accessed: 2019-12-10.

- [4] Chainarong Amornbunchornvej, Ivan Brugere, Ariana Strandburg-Peshkin, Damien Farine, Margaret C Crofoot, and Tanya Y Berger-Wolf. 2018. Coordination Event Detection and Initiator Identification in Time Series Data. *ACM Trans. Knowl. Discov. Data* 12, 5, Article 53 (6 2018), 33 pages. <https://doi.org/10.1145/3201406>
- [5] Chainarong Amornbunchornvej, Elena Zheleva, and Tanya Berger-Wolf. 2019. Variable-lag Granger Causality for Time Series Analysis. In *2019 IEEE International Conference on Data Science and Advanced Analytics (DSAA)*. IEEE, 21–30. <https://doi.org/10.1109/DSAA.2019.00016>
- [6] Andrew Arnold, Yan Liu, and Naoki Abe. 2007. Temporal Causal Modeling with Graphical Granger Methods. In *Proceedings of the 13th ACM SIGKDD International Conference on Knowledge Discovery and Data Mining (KDD '07)*. ACM, New York, NY, USA, 66–75. <https://doi.org/10.1145/1281192.1281203>
- [7] Erdal Atukeren et al. 2010. The relationship between the F-test and the Schwarz criterion: implications for Granger-causality tests. *Econ Bull* 30, 1 (2010), 494–499.
- [8] Adelchi Azzalini and Adrian W Bowman. 1990. A look at some data on the Old Faithful geyser. *Journal of the Royal Statistical Society: Series C (Applied Statistics)* 39, 3 (1990), 357–365.
- [9] Lionel Barnett, Adam B. Barrett, and Anil K. Seth. 2009. Granger Causality and Transfer Entropy Are Equivalent for Gaussian Variables. *Phys. Rev. Lett.* 103 (Dec 2009), 238701. Issue 23. <https://doi.org/10.1103/PhysRevLett.103.238701>
- [10] Simon Behrendt, Thomas Dimpfl, Franziska J. Peter, and David J. Zimmermann. 2019. RTransferEntropy fi!? Quantifying information flow between different time series using effective transfer entropy. *SoftwareX* 10 (2019), 100265. <https://doi.org/10.1016/j.softx.2019.100265>
- [11] George EP Box, Gwilym M Jenkins, Gregory C Reinsel, and Greta M Ljung. 2015. *Time series analysis: forecasting and control*. John Wiley & Sons.
- [12] Bernard Chazelle. 2011. The Total s-Energy of a Multiagent System. *SIAM Journal on Control and Optimization* 49, 4 (2011), 1680–1706. <https://doi.org/10.1137/100791671> arXiv:<https://doi.org/10.1137/100791671>
- [13] Yonghong Chen, Govindan Rangarajan, Jianfeng Feng, and Mingzhou Ding. 2004. Analyzing multiple nonlinear time series with extended Granger causality. *Physics Letters A* 324, 1 (2004), 26–35.
- [14] Margaret C Crofoot, Roland W Kays, and Martin Wikelski. 2015. Data from: Shared decision-making drives collective movement in wild baboons.
- [15] Michael Eichler. 2013. Causal inference with multiple time series: principles and problems. *Philosophical Transactions of the Royal Society A: Mathematical, Physical and Engineering Sciences* 371, 1997 (2013), 20110613. <https://doi.org/10.1098/rsta.2011.0613>
- [16] Michael Eichler. 2013. Causal inference with multiple time series: principles and problems. *Philosophical Transactions of the Royal Society A: Mathematical, Physical and Engineering Sciences* 371, 1997 (2013), 20110613.
- [17] Toni Giorgino et al. 2009. Computing and visualizing dynamic time warping alignments in R: the dtw package. *Journal of statistical Software* 31, 7 (2009), 1–24.
- [18] Clive WJ Granger. 1969. Investigating causal relations by econometric models and cross-spectral methods. *Econometrica: Journal of the Econometric Society* (1969), 424–438.
- [19] Théophile Griveau-Billion and Ben Calderhead. 2019. Efficient structure learning with automatic sparsity selection for causal graph processes. *arXiv preprint arXiv:1906.04479* (2019).
- [20] Akane Iseki, Y. Mukuta, Y. Ushiki, and T. Harada. 2019. Estimating the causal effect from partially observed time series. In *AAAI*.
- [21] Dominik Janzing and Bernhard Scholkopf. 2010. Causal inference using the algorithmic Markov condition. *IEEE Transactions on Information Theory* 56, 10 (2010), 5168–5194.
- [22] Eamonn J Keogh and Michael J Pazzani. 2001. Derivative dynamic time warping. In *Proceedings of the 2001 SIAM international conference on data mining*. SIAM, 1–11.
- [23] Joon Lee, Shamim Nemati, Ikaro Silva, Bradley A Edwards, James P Butler, and Atul Malhotra. 2012. Transfer entropy estimation and directional coupling change detection in biomedical time series. *Biomedical engineering online* 11, 1 (2012), 19.
- [24] Yan Liu, Taha Bahadori, and Hongfei Li. 2012. Sparse-gev: Sparse latent space model for multivariate extreme value time serie modeling. In *ICML*.
- [25] Daniel Malinsky and Peter Spirtes. 2018. Causal structure learning from multivariate time series in settings with unmeasured confounding. In *Proceedings of 2018 ACM SIGKDD Workshop on Causal Discovery*. 23–47.
- [26] Abdullah Mueen and Eamonn Keogh. 2016. Extracting Optimal Performance from Dynamic Time Warping. In *Proceedings of the 22Nd ACM SIGKDD International Conference on Knowledge Discovery and Data Mining (KDD '16)*. ACM, New York, NY, USA, 2129–2130. <https://doi.org/10.1145/2939672.2945383>
- [27] J Pearl. 2000. *Causality: Models, reasoning and inference* Cambridge University Press. Cambridge, MA, USA, 9 (2000).
- [28] Wei Peng, Tong Sun, Philip Rose, and Tao Li. 2007. A Semi-automatic System with an Iterative Learning Method for Discovering the Leading Indicators in Business Processes. In *Proceedings of the 2007 International Workshop on Domain Driven Data Mining (DDDM '07)*. ACM, New York, NY, USA, 33–42. <https://doi.org/10.1145/1288552.1288557>

- [29] Jonas Peters, Dominik Janzing, and Bernhard Schölkopf. 2013. Causal inference on time series using restricted structural equation models. In *Advances in Neural Information Processing Systems*. 154–162.
- [30] C. J. Quinn, N. Kiyavash, and T. P. Coleman. 2015. Directed Information Graphs. *IEEE Transactions on Information Theory* 61, 12 (Dec 2015), 6887–6909. <https://doi.org/10.1109/TIT.2015.2478440>
- [31] Hiroaki Sakoe and Seibi Chiba. 1978. Dynamic programming algorithm optimization for spoken word recognition. *IEEE transactions on acoustics, speech, and signal processing* 26, 1 (1978), 43–49.
- [32] Bernhard Schölkopf, Dominik Janzing, Jonas Peters, Eleni Sgouritsa, Kun Zhang, and Joris Mooij. 2012. On causal and anticausal learning. In *ICML*.
- [33] Thomas Schreiber. 2000. Measuring information transfer. *Physical review letters* 85, 2 (2000), 461.
- [34] Patrick Schwab, Djordje Miladinovic, and Walter Karlen. 2019. Granger-causal attentive Mixtures of Experts: Learning Important Features with Neural Networks. In *AAAI*.
- [35] Naji Shajarisales, Dominik Janzing, Bernhard Schölkopf, and Michel Besserve. 2015. Telling cause from effect in deterministic linear dynamical systems. In *ICML*. 285–294.
- [36] C. E. Shannon. 1948. A mathematical theory of communication. *The Bell System Technical Journal* 27, 3 (July 1948), 379–423. <https://doi.org/10.1002/j.1538-7305.1948.tb01338.x>
- [37] Shengjia Shao, Ce Guo, Wayne Luk, and Stephen Weston. 2014. Accelerating transfer entropy computation. In *2014 International Conference on Field-Programmable Technology (FPT)*. IEEE, 60–67.
- [38] Takashi Shibuya, Tatsuya Harada, and Yasuo Kuniyoshi. 2009. Causality quantification and its applications: structuring and modeling of multivariate time series. In *KDD*. ACM.
- [39] Elsa Siggiridou and Dimitris Kugiumtzis. 2016. Granger causality in multivariate time series using a time-ordered restricted vector autoregressive model. *IEEE Transactions on Signal Processing* 64, 7 (2016), 1759–1773.
- [40] Amy Sliva, Scott Neal Reilly, Randy Casstevens, and John Chamberlain. 2015. Tools for validating causal and predictive claims in social science models. *Procedia Manufacturing* 3 (2015), 3925–3932.
- [41] Peter Spirtes, Clark Glymour, and Richard Scheines. 1993. *Discovery Algorithms for Causally Sufficient Structures*. Springer New York, New York, NY, 103–162. https://doi.org/10.1007/978-1-4612-2748-9_5
- [42] A. Strandburg-Peshkin and et al. 2013. Visual sensory networks and effective information transfer in animal groups. *Current Biology* 23, 17 (2013), R709–R711.
- [43] Ariana Strandburg-Peshkin, Damien R Farine, Iain D Couzin, and Margaret C Crofoot. 2015. Shared decision-making drives collective movement in wild baboons. *Science* 348, 6241 (2015), 1358–1361.
- [44] Youqiang Sun, Jiuyong Li, Jixue Liu, Christopher Chow, Bingyu Sun, and Rujing Wang. 2015. Using causal discovery for feature selection in multivariate numerical time series. *Machine Learning* 101, 1 (01 Oct 2015), 377–395. <https://doi.org/10.1007/s10994-014-5460-1>
- [45] Hal R. Varian. 2016. Causal inference in economics and marketing. *Proceedings of the National Academy of Sciences* 113, 27 (2016), 7310–7315. <https://doi.org/10.1073/pnas.1510479113> arXiv:<https://www.pnas.org/content/113/27/7310.full.pdf>
- [46] Tao Yuan, Gang Li, Zhaohui Zhang, and S Joe Qin. 2016. Deep causal mining for plant-wide oscillations with multilevel Granger causality analysis. In *American Control Conference (ACC), 2016*. IEEE, 5056–5061.